RAPID COMMUNICATIONS

PHYSICAL REVIEW B VOLUME 44, NUMBER 18 1 NOVEMBER 1991-II

Phonon-limited resistivity of high-T_c oxides: A strong-coupling calculation

R. Zeyher

Max-Planck-Institut für Festkörperforschung, 7 Stuttgart 80, Federal Republic of Germany

(Received 21 May 1991; revised manuscript received 4 September 1991)

The equations of the lowest-order conserving Green's-function approximation for the phonon-limited resistivity are solved numerically. The input functions $\alpha^2F(\omega)$ and $\alpha^2_{tr}F(\omega)$ are calculated from a screened ionic model for $YBa_2Cu_3O_7$ and lead to integrated coupling constants $\lambda\sim 3$ and $\lambda_{tr}\sim 1$. The calculated temperature dependence of the resistivity and the width of the Drude peak as well as the absolute values of the prefactors are in excellent agreement with experiment. This result shows, in particular, that the observed resistivity in high-T_c oxides does not imply a weak electron-phonon coupling.

The normal-state resistivity ρ of most high-temperature superconductors is linear in temperature to a high accuracy.[1-3] At present there is no generally accepted explanation for this linear behavior nor a consensus about the nature of the scatterers. A linear temperature dependence has so far been obtained theoretically only in the form of leading terms in high- or low-temperature expansions so that the linear law holds only above or below a certain characteristic temperature. Why this characteristic temperature is so low and of the order of T_c represents a puzzle for most theories working with high-temperature expansions.

In the case of phonon-limited resistivity the characteristic energy for the crossover to a linear temperature dependence is the Debye energy or the energy of a representative optical phonon. At first sight this energy also seems to be too large to be able to explain the observed linear dependence down to T_c. However, it has been shown in the case of the Bloch-Grüneisen approximation to the Boltzmann equation that the crossover energy may be substantially lower than the Debye energy.[4,5] On the other hand, the same calculations lead to the conclusion that the observed slope of the resistivity is compatible only with a weak electron-phonon coupling. For instance, a value of about 0.2 for the dimensionless coupling constant λ has been deduced for $YBa_2Cu_3O_7$, assuming that the whole temperature-dependent part of the resistivity is due to electron-phonon scattering.[5] An even smaller upper bound for λ of 0.08 has been obtained for $Bi_{2+x}Sr_{2-y}CuO_{6\pm\delta}$.[1] Such small values for λ can yield only very small values for T_c. Therefore it was widely concluded that the electron-phonon coupling is irrelevant for high-T_c superconductivity.

The above arguments, based on weak-coupling ideas, may, however, be invalid if high-T_c oxides are characterized by a strong electron-phonon coupling. To be able to decide whether a strong electron-phonon coupling is compatible with the observed ρ or not needs an approximation which also covers the strong-coupling case. One possibility for such a treatment is the lowest-order conserving approximation[6] which we will study in this paper. Higher-order contributions are smaller by the Migdal ratio ω_{ph}/E_F (ω_{ph} is a typical phonon energy, E_F the Fermi energy) and thus may be omitted.

The dc conductivity can be calculated in the lowest-order conserving approximation from the following equations:[7,8]

$$\sigma=-\frac{ne^2}{2m}\int_{-\infty}^{\infty}d\varepsilon\frac{dn_F(\varepsilon)}{d\varepsilon}\frac{\Lambda(\varepsilon)}{\Gamma(\varepsilon)}, \tag{1}$$

$$\Gamma(\varepsilon)=\pi\int_0^{\omega_{max}}du\,\alpha^2F(u)[2n_B(u)+n_F(\varepsilon+u)+n_F(u-\varepsilon)], \tag{2}$$

$$\Lambda(\varepsilon)=1+\pi\int_0^{\omega_{max}}du[\alpha^2F(u)-\alpha^2_{tr}F(u)]\left[[n_B(u)+n_F(\varepsilon+u)]\frac{\Lambda(\varepsilon+u)}{\Gamma(\varepsilon+u)}+[n_B(u)+n_F(u-\varepsilon)]\frac{\Lambda(\varepsilon-u)}{\Gamma(\varepsilon-u)}\right]. \tag{3}$$

n and m are the density and the mass of the charge carriers, respectively. ω_{max} denotes the maximal phonon frequency. n_B and n_F are the Bose and Fermi distribution functions, respectively. The two functions α^2F and α^2F_{tr} are defined by[7]

$$\alpha^2F(u)=N(0)\sum_\lambda\langle\langle|g_{pp'\lambda}|^2\delta[u-\omega(^{p-p'}_{\lambda})]\rangle_p\rangle_{p'}, \tag{4}$$

$$\alpha^2_{tr}F(u)=N(0)\sum_\lambda\langle\langle|g_{pp'\lambda}|^2\frac{(p-p')^2_{\|}}{2k_F^2}\delta[u-\omega(^{p-p'}_{\lambda})]\rangle_p\rangle_{p'}, \tag{5}$$

where $N(0)$ is the density of hole states for one spin direction at the Fermi energy. $N(0)$ has incorporated all renormalization effects due to the electron-electron interaction, but is unrenormalized with respect to the hole-phonon interaction. $\omega(^{\mathbf{p}}_{\lambda})$ is the frequency of the phonon with branch index λ and momentum $\mathbf{p}$. $\langle\cdots\rangle_{\mathbf{p}}$ denotes an average over the Fermi surface with respect to the momentum $\mathbf{p}$. $g_{\mathbf{pp}'\lambda}$ stands for the fully renormalized electron-phonon interaction. $(\mathbf{p}-\mathbf{p}')_{\|}$ is the projection of the vector $\mathbf{p}-\mathbf{p}'$ onto the plane which accounts for the fact that the Fermi velocity is nonzero only parallel to the plane in our model. Λ and Γ denote the vertex function and the negative imaginary part of the self-energy, respectively.

For the following it is convenient to recast Eq. (1) into the standard form

$$\rho=\frac{4\pi}{\Omega_{\mathrm{pl}}^{*2}}\frac{1}{\tau^*} \tag{6}$$

with

$$\Omega_{\mathrm{pl}}^{*2}=\frac{4\pi e^2 n}{(1+\lambda)m}\,, \tag{7}$$

$$\tau^*=-\frac{1+\lambda}{2}\int_{-\infty}^{\infty}d\varepsilon\frac{dn_F(\varepsilon)}{d\varepsilon}\frac{\Lambda(\varepsilon)}{\Gamma(\varepsilon)}\,, \tag{8}$$

$$\lambda=2\int_0^{\infty}du\frac{\alpha^2F(u)}{u}\,. \tag{9}$$

ρ is the resistivity and equal to $1/\sigma$. Equations (7) and (8) define the squared plasmon frequency and the transport relaxation time of dressed particles containing renormalization effects resulting from the electron-phonon interaction. The usefulness of Eq. (6) lies in the fact that the inverse transport lifetime of dressed particles $1/\tau^*$ can be measured approximately as the width of the Drude peak if $T\ll\bar{\omega}$, where $\bar{\omega}$ is an average phonon frequency defined in Eq. (11) [for $T\gg\bar{\omega}$, λ should be dropped in Eq. (8) because of the shakeoff of phonon renormalizations due to temperature]. Thus, both the dynamic part $1/\tau^*$ and the static part Ω_{pl}^* can be determined independently from experiment and compared with theory. Equation (9) represents the usual definition of the dimensionless coupling constant λ.

Before presenting numerical results we perform a high-temperature expansion of Eqs. (1)–(3) and assume that βu (but not $\beta\varepsilon$) is small compared to one. The expansion for $\Gamma(\varepsilon)$ is straightforward and yields

$$\Gamma(\varepsilon)=\pi\lambda\left[T+\frac{\beta\bar{\omega}^2}{12}\left(1-\frac{3}{\cosh^2(\beta\varepsilon/2)}\right)+\cdots\right] \tag{10}$$

with the definition

$$\bar{\omega}^2=\frac{2}{\lambda}\int_0^{\infty}du\,u\alpha^2F(u)\,. \tag{11}$$

Expanding Eq. (3) in powers of β one obtains after some algebra

$$\Lambda(\varepsilon)=\frac{\lambda}{\lambda_{\mathrm{tr}}}\left[1-\frac{\beta^2}{12}(\bar{\omega}_{\mathrm{tr}}^2-\bar{\omega}^2)\times\left(1-\frac{3}{\cosh^2(\beta\varepsilon/2)}\right)+\cdots\right]. \tag{12}$$

Expanding, finally, Eq. (8) we find

$$\frac{1}{\tau^*}=2\pi T\frac{\lambda_{\mathrm{tr}}}{1+\lambda}\left[1-\frac{\beta^2}{12}\bar{\omega}_{\mathrm{tr}}^2+\cdots\right]. \tag{13}$$

λ_{tr} and $\bar{\omega}_{\mathrm{tr}}^2$ are defined by Eqs. (9) and (11), respectively, with α^2F replaced by α_{tr}^2F. The first two terms shown explicitly on the right-hand side of Eq. (13) agree with the corresponding ones in the high-temperature expansion of the Bloch-Grüneisen formula of $(1+\lambda)/\tau^*$, see Eq. (20) of Ref. 9. From Eqs. (4), (5), and (9) it follows that $\lambda_{\mathrm{tr}}=\lambda$ if both $g_{\mathbf{pp}'\lambda}$ and $\omega(^{\mathbf{p}}_{\lambda})$ are independent of momentum. The prefactor $\lambda_{\mathrm{tr}}/(1+\lambda)$ in Eq. (13) then approaches 1 in the strong-coupling limit. However, for a momentum-dependent coupling function this prefactor tends to $\lambda_{\mathrm{tr}}/\lambda$ in the strong-coupling limit which may be small if vertex corrections are important.

We have calculated α^2F and α_{tr}^2F for $YBa_2Cu_3O_7$ using the screened ionic model of Ref. 10. Local-field effects for wave vectors perpendicular to the planes now also are included exactly. In view of recent photoemission data[11] we used in our calculations the larger value $2k_F=1$ Å^{-1} instead of $2k_F=0.7$ Å^{-1} as in Ref. 10. The long-range forces are more efficiently screened with increasing k_F leading to a reduction of the α^2F values for a fixed Coulomb enhancement factor Z_c. The diagrams in Fig. 1 show the calculated functions $\alpha^2F(\omega)$ and $\alpha_{\mathrm{tr}}^2F(\omega)$ using $2k_F=1$ Å^{-1}, $Z_c=3.5$,[12] a sampling with 512 $\mathbf{k}$ points in the little Brillouin zone, and a channel width of 2 meV. Compared to the density of phonon states (see upper diagram of Fig. 1 of Ref. 10) α^2F and α_{tr}^2F give a larger weight to high-frequency phonons which produce large

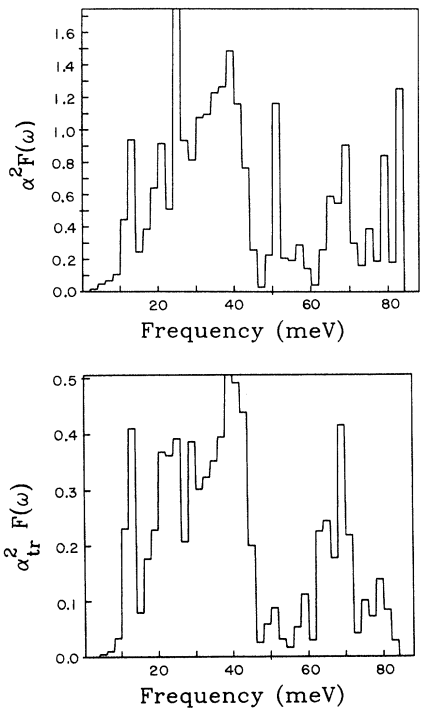

FIG. 1. Calculated $\alpha^2F(\omega)$ (upper part) and $\alpha_{\mathrm{tr}}^2F(\omega)$ (lower part) for $YBa_2Cu_3O_7$.

Coulomb potentials and, therefore, large changes in the local chemical potentials. The dimensionless coupling strengths, corresponding to the functions in Fig. 1, are $\lambda=3.07$ and $\lambda_{tr}=1.08$ (the quoted value for λ in Ref. 10 is too small by a factor of 2 because of a mistake). The resulting small ratio for λ_{tr}/λ may be surprising because it is near one in many metals.[13] In our case, the smallness of this ratio seems to be caused mainly by the substantial momentum dependence of the electron-phonon coupling functions of the screened ionic model. The absolute values for $\alpha^2F(\omega)$ and $\alpha^2_{tr}F(\omega)$ are subject to some uncertainty. The details of the band structure and geometry of the Fermi surface are not taken into account realistically in our tight-binding calculation with only nearest-neighbor interactions. Furthermore, the Fermi-liquid corrections renormalize the density-of-states factor in α^2F and $\alpha^2_{tr}F$ in the simple way $N(0)\rightarrow N(0)Z_c$ only if one assumes that the cancellation of the Coulomb vertex and Z_c takes place for all relevant momenta and frequencies and not just in the hydrodynamic limit.

Figure 2 shows the real and imaginary parts of the self-energy $\Sigma(k_F,\varepsilon)$ of electrons for $T=100$ K (solid curves) and $T=300$ K (dashed curves) resulting from the electron-phonon interaction. At very low temperatures and small frequencies the negative imaginary part of Σ, $\Gamma(\varepsilon)$, is proportional to T^2 for $\varepsilon=0$ and to ε^3 for $T=0$ in accordance with Fermi-liquid theory. $\Gamma(\varepsilon=0)$ increases quadratically in temperature up to about 150 K and then switches to a linear law. For a fixed temperature $\Gamma(\varepsilon)$ increases first quadratically in ε within a small interval $0<\varepsilon<20$ meV, then turns over to a quasilinear law and saturates above the largest phonon frequency ω_{max}. In the normal state $\Gamma(\varepsilon)$ is larger or comparable to the energy ε up to $\varepsilon\sim150$ meV. The width of dressed particles Γ^* is given by Γ/Z_{ph}. At small energies Z_{ph} is about 4 and then decreases monotonically to 1 on a phonon scale. As a result Γ^* is somewhat smaller than ε at 100 K, but not at 300 K. This indicates that a quasiparticle description for the holes may no longer be adequate at higher temperatures.

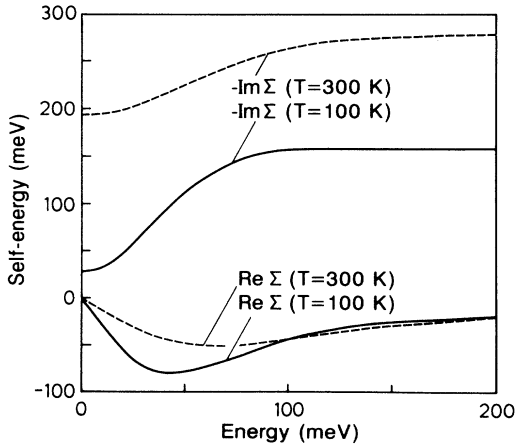

FIG. 2. Real and imaginary parts of the self-energy of electrons at $k=k_F$ for $T=100$ K (solid lines) and $T=300$ K (dashed lines).

Figure 3 shows solutions of the vertex function $\Lambda(\varepsilon)$ obtained by iterating the integral equation (3). The solid, dotted, and dashed lines correspond to $T=100$, 200, and 300 K, respectively. According to our high-temperature expansion Λ approaches the energy-independent value λ/λ_{tr} at high temperatures which is about 3 in our case. The scattering with phonons then can be considered as a quasistatic process. The dashed curve in Fig. 3 corresponds approximately to this case. For $T=200$ K, and especially $T=100$ K, $\Lambda(\varepsilon)$ depends strongly on energy: it increases below ω_{max}, reaches a maximum at about ω_{max}, and then decays towards a finite asymptotic value Λ_∞ at high energies.

Figure 4 shows the calculated temperature dependence of the renormalized transport relaxation rate $1/\tau^*$. The curve is linear between $T_c\sim90$ and 400 K to a very high accuracy. This quasilinear behavior, however, cannot be identified with the true asymptotic law of the high-temperature expansion: If extrapolated down to $T=0$, one finds a finite negative instead of a vanishing intercept. The resistivity curve exhibits a very smooth and gradual decrease in the slope at temperatures larger than 400 K until the true asymptotic linear law is reached at $T>\omega_{max}\sim1000$ K. Performing the above calculations just for one oscillator with a frequency ω_0, we find a crossover temperature to a linear behavior already near $\omega_0/3$, rather independently of the coupling strength or the ratio λ_{tr}/λ. Such a property also seems to underlie the linear law in Fig. 4.

The slope of the resistivity curve between 100 and 400 K is practically identical with the asymptotic slope at high temperatures and thus is given by $2\pi T\lambda_{tr}/(1+\lambda)$. Using our values $\lambda=3.07$ and $\lambda_{tr}=1.08$ we obtain $\tau^{*-1}=1.66$ T, which is in excellent agreement with the observed value[14] 1.9 T. Important for this good agreement is the small ratio λ_{tr}/λ in the screened ionic model. For $\lambda_{tr}=\lambda$ the experimental value of the slope would imply $\lambda\sim0.2$, so essentially we would be back at the arguments of Ref. 5 in favor of a weak electron-phonon coupling. The saturation argument of Ref. 1 does not apply in our case: The transport lifetime τ^* for quasiparticles is much larger than the lifetime of particles. Using the observed mass $5m_e$,[15] we obtain a Fermi velocity of about 1.2×10^7

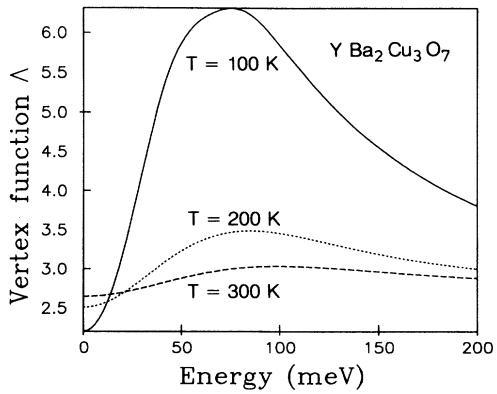

FIG. 3. Energy dependence of the vertex function Λ for three different temperatures.

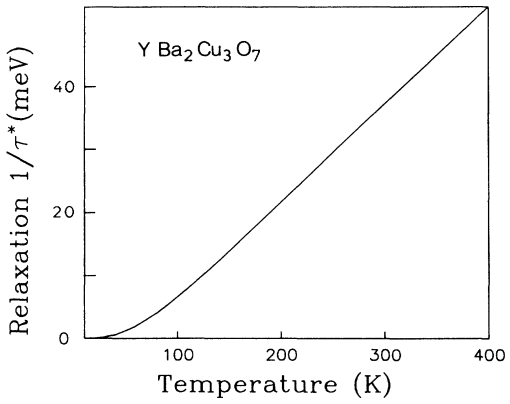

FIG. 4. Calculated renormalized transport relaxation rate $1/\tau^*$ as a function of temperature.

cm/sec and a free mean path of about 20 Å at 300 K which is much larger than interatomic distances.

Experimental data also allow us to check the static quantity $\Omega_{\rm pl}^*$. Since our calculation does not include a chain contribution we should compare it with ρ_a, the resistivity along the a direction in untwinned $YBa_2Cu_3O_7$. Assuming that the lowest value for ρ in Refs. 2 and 3 corresponds to the best sample we have $\rho_a = \alpha T$ with $\alpha = 0.6$ $\mu\Omega\,{\rm cm\,K}^{-1}$ (Ref. 3, sample A). Dividing now ρ_a by Schlesinger's $1/\tau^*$ we find $(\Omega_{\rm pl}^*)_{\rm expt} \sim 1.4$ eV. On the other hand, band-structure calculations[9] yield the bare value $\Omega_{\rm pl} \sim 2.9$ eV so that $(\Omega_{\rm pl}^*)_{\rm theor} \sim 2.9/\sqrt{1+\lambda}$ eV ~ 1.4 eV, again in excellent agreement with the experimental value.

Finally, we would like to point out a severe constraint for any nonphonon-scattering mechanism for ρ. Assume that the linear temperature dependence in ρ is due to a nonphonon mechanism. Since ρ is approximately additive in different scattering mechanisms, only a very small additional phonon contribution to ρ could be tolerated in view of the nearly perfect linear law. If one then assumes that $\lambda_{\rm tr}/\lambda$ is of the order of $\frac{1}{3}$ or larger, Eq. (13) implies implausible small values for λ. The conclusion is that either the electron-phonon interaction is inactive because of the presence of some unknown process or the assumption of a nonphonon-scattering process has to be dropped.

The author thanks J. Keller, G. F. Maksimov, and A. B. Kaiser for useful hints and P. B. Allen for very helpful discussions on several topics of this paper.

[1]S. Martin, A. T. Fiory, R. M. Fleming, L. F. Schneemeyer, and J. V. Waszczak, Phys. Rev. B **41**, 846 (1990).
[2]U. Welp, S. Fleshler, W. K. Kwok, J. Downey, Y. Fang, G. W. Crabtree, and J. Z. Liu, Phys. Rev. B **42**, 10189 (1990).
[3]T. A. Friedmann, M. W. Rabin, J. Giapintzakis, J. P. Rice, and D. M. Ginsberg, Phys. Rev. B **42**, 6217 (1990).
[4]R. Micnas, J. Ranninger, and S. Robaszkiewicz, Phys. Rev. B **36**, 4051 (1987).
[5]D. Y. Xing, M. Liu, and C. S. Ting, Phys. Rev. B **37**, 9769 (1988).
[6]G. Baym, Phys. Rev. **127**, 1391 (1962).
[7]G. D. Mahan, *Many-Particle Physics* (Plenum, New York, 1981).
[8]T. Holstein, Ann. Phys. (N.Y.) **29**, 410 (1964).
[9]P. B. Allen, W. E. Pickett, and H. Krakauer, Phys. Rev. B **37**, 7482 (1988).
[10]R. Zeyher, Z. Phys. B **80**, 187 (1990).
[11]J. C. Campuzano, G. Jennings, M. Faiz, L. Beaulaigue, B. W. Veal, J. Z. Liu, A. P. Paulikas, K. Vandervoort, H. Claus, R. S. List, A. J. Arko, and R. J. Bartlett, Phys. Rev. Lett. **64**, 2308 (1990).
[12]G. Mante, R. Claessen, T. Buslaps, S. Harm, R. Manzke, M. Skibowski, and J. Fink, Z. Phys. B **80**, 181 (1990).
[13]P. B. Allen, Phys. Rev. B **36**, 2920 (1987).
[14]Z. Schlesinger, R. T. Collins, F. Holtzberg, C. Feild, S. H. Blanton, U. Welp, G. W. Crabtree, Y. Fang, and J. Z. Liu, Phys. Rev. Lett. **65**, 801 (1990).
[15]A. T. Fiory, A. F. Hebard, R. H. Eick, P. M. Mankiewich, R. E. Howard, and M. L. O'Malley, Phys. Rev. Lett. **65**, 3441 (1990).